Melanocortin-1 Receptor-Targeting With Radiolabeled Cyclic α-Melanocyte-Stimulating Hormone Analogs for Melanoma Imaging

Paula D. Raposinho, João D. G. Correia, Maria Cristina Oliveira, Isabel Santos
Unidade de Ciências Químicas e Radiofarmacêuticas, ITN, Estrada Nacional 10, 2686-953 Sacavém, Portugal

Received 20 February 2010; revised 21 April 2010; accepted 29 April 2010
Published online 4 August 2010 in Wiley Online Library (wileyonlinelibrary.com). DOI 10.1002/bip.21490

ABSTRACT:

Melanoma is a type of skin cancer known for its high aggressiveness, early dissemination of metastases, and poor prognosis once metastasized. Thus, early diagnosis of melanoma is a key issue for increasing patient survival. The overexpression of melanocortin-1 receptors (MC1R) in isolated melanoma cells and melanoma tissues led to the radiolabeling of several linear and cyclic MC analogs for melanoma imaging or therapy. Cyclization of α-melanocyte stimulating hormone (α-MSH) peptides has been successfully used to improve binding affinity and in vivo stability of peptides. Herein, we describe the different peptide cyclization strategies recently reported for radiolabeled α-MSH analogs and discuss how such strategies affect MC1R binding affinity, pharmacokinetic profile, and MC1R-melanoma imaging. This review also highlights how the nature of the radiometal and labeling approach influence those properties. Among the cyclized α-MSH peptides reported, ^{99m}Tc/^{111}In-labeled metal-cyclized and lactam bridge–cyclized peptides displayed the highest melanoma and lowest renal uptake values in B16/F1 melanoma-bearing mice and became the most promising tools to be further explored as potential melanoma imaging probes. © *2010 Wiley Periodicals, Inc. Biopolymers (Pept Sci) 94: 820–829, 2010.*

Keywords: *melanoma; melanocortin type 1 receptor; radionuclides; imaging; cyclic peptides; nuclear medicine*

Correspondence to: Paula D. Raposinho; e-mail: paular@itn.pt

This article was originally published online as an accepted preprint. The "Published Online" date corresponds to the preprint version. You can request a copy of the preprint by emailing the Biopolymers editorial office at biopolymers@wiley.com

INTRODUCTION

Malignant melanoma is the most lethal form of skin cancer and the most commonly diagnosed malignancy among young adults with an increasing incidence.[1,2] Representing only 5% of all skin cancer types, melanoma contributes to more than 50% to all skin cancer deaths. Because of its aggressivity, high metastatic potential, and resistance to cytotoxic agents, the improvement of melanoma patient survival relies on an early diagnosis, along with an accurate staging of disease extension. Despite limitations in terms of sensitivity and specificity, ^{18}F-fluoro-deoxy-glucose is widely used in melanoma positron emission tomography (PET) staging, providing useful information for the detection of distal organ metastases.[3,4] To overcome ^{18}F-fluoro-deoxy-glucose limitations, many radiocompounds have been synthesized and evaluated as molecular imaging agents for melanoma detection. However, so far, no significant results were obtained; there still exists a great need of novel and effective imaging probes for its detection. Most of the research underway in radiopharmaceutical sciences has shown that peptide receptor–targeting in vivo is a successful method to image and treat various types of cancer.[5] The best example of such an approach was the successful somatostatin receptor–targeting with radiolabeled somatostatin analogs, now routinely used in the clinic.[6] Concerning melanoma, it is also known that both melanotic and amelanotic murine and human melanomas overexpress the melanocortin type 1 receptor (MC1R), a member of the G protein-coupled receptors family.[7–9] Furthermore, more than 80% of human metastatic melanoma samples have also been identified to display MC1R receptors. α-Melanocyte stimulating hormone (α-MSH), a tridecapep-

Table I Structure of α-MSH and Some α-MSH Analogs

Peptide	Amino acids
Ac-Ser-Tyr-Ser- Met[4]-Glu[5]-His-Phe[7]-Arg-Trp-Gly-Lys-Pro-Val-NH_2 (**α-MSH**)	13
Ac-Ser-Tyr-Ser-**Nle**[4]-Glu[5]-His-D-**Phe**[7]-Arg-Trp-Gly-Lys-Pro-Val-NH_2 (**NDP-MSH**)	**13**
Ac-**Nle**[4]-**Asp**[5]-His-D-**Phe**[7]-Arg-Trp-Gly-Lys-NH_2 (**NAPamide**)	**8**
Ac-**Cys**[3]-**Cys**[4]-Glu[5]-His-D-**Phe**[7]-Arg-Trp-**Cys**[10]-Lys-Pro-Val-NH_2 (**CCMSH**)	**11**
Ac-**Cys**[3]-**Cys**[4]-Glu[5]-His-D-**Phe**[7]-Arg-Trp-**Cys**[10]-Arg^{11}-Pro-Val-NH_2 (**CCMSH(Arg[11])**)	**11**
Ac-**cyclo[Cys**[4]-Glu[5]-His-D-**Phe**[7]-Arg-Trp-**Cys**[10]]-Lys-Pro-Val-NH_2 (**CMSH**)	**10**
Ac-**Nle**[4]-**cyclo[Asp**[5]-His-D-**Phe**[7]-Arg-Trp-**Lys**[10]]-NH_2 (**Melanotan-II: MTII**)	**7**
βAla[3]-**Nle**[4]-**cyclo[Asp**[5]-His-D-**Phe**[7]-Arg-Trp-**Lys**[10]]-NH_2 (***β*AlaMT-II**)	**8**
βAla[3]-**Nle**[4]-**Asp**[5]-His-*D*Phe[7]-Arg-Trp-**Lys**[10]-NH_2 (**MSHoct**)	**8**

tide (Table I), is the most potent naturally occurring melanotropic peptide for the activation of MC1R but, like many other endogenous peptides, presents a short half-life in humans.[10] Structure–bioactivity studies have shown that the minimal sequence of α-MSH required for biological activity is His-Phe-Arg-Trp and that the replacement in α-MSH of Met^4 and Phe^7 by Nle and D-Phe, respectively, leads to the potent [Nle^4,*D*Phe^7]-αMSH analog (NDP-MSH, mean inhibitory concentration (IC_{50}) = 0.21 n*M*) (Tables I and II), which is enzymatically stable and has a long half-life.[10] The short linear peptide [Ac-Nle^4,Asp^5,D-Phe^7]-αMSH_{4-11} (NAPamide) also displays high affinity for MC1R (IC_{50} = 0.27 n*M*). The αMSH analogs side chain to side chain cyclized, either via disulfide- (e.g. [$Cys^{4,10}$, *D*Phe^7]α-MSH, CMSH; Table I) or lactam-bridge (e.g., MTII, Tables I and II), have also shown increased receptor binding affinity and resistance to proteolysis.[10–12]

Taking advantage of the knowledge gained in structure–bioactivity studies for the MC system (α-MSH analogs/MC receptors), a great deal of effort has been directed toward the development of radiolabeled analogs of α-MSH for both diagnosis and therapy of melanoma. Stable α-MSH peptide analogs with

Table II MC1R Affinity of α-MSH Analogs and Their Chelator–Peptide Conjugates

Peptide or Chelator–Peptide Conjugate	IC_{50} (nM)[a]	Ref.
α-MSH (endogenous peptide)	1.65 ± 0.18	47
NDP ((linear)	0.21 ± 0.03	33
DOTA-NDP (linear)	0.22 ± 0.02	33
NAPamide	0.27 ± 0.07	11
DOTA-NAPamide	1.37 ± 0.35	11
NAPamide	0.78 ± 0.03	44
Pz1-NAPamide	0.66 ± 0.13	44
CCMSH (linear)	7.6	34
DOTA-CCMSH (linear)	4.9 ± 2.6	33
Re-CCMSH (cyclic)	2.9	34
DOTA-Re-CCMSH (cyclic)	1.2 ± 0.3	33
DOTA-Re-CCMSH(Arg^{11}) (cyclic)	2.1	36
Cu-DOTA-Re-CCMSH(Arg^{11}) (cyclic)	6.9	38
Cu-CBTE2A-Re-CCMSH(Arg^{11}) (cyclic)	5.4 ± 0.59	39
Ac-*D*Lys(^{19}F-FB)-Re-CCMSH(Arg^{11}) Iso I	5.7 ± 0.7	16
Ac-*D*Lys(^{19}F-FB)-Re-CCMSH(Arg^{11}) Iso II	9.0 ± 1.0	
MSHoct (linear)	1.25 ± 0.08	11
Pz1-MSHoct (linear)	1.25 ± 0.66	Raposinho et al. (unpublished results)
pz1-*β*AlaMT-II (lactam-cyclized)	0.21 ± 0.05	Raposinho et al. (unpublished results)
DOTA-CycMSH (lactam-cyclized)	1.75	45
DOTA-GlyGlu-CycMSH (lactam-cyclized)	0.90	45
Ac-GluGlu-CycMSH[DOTA] (lactam-cyclized)	0.60	47

[a]IC_{50} values were evaluated by competition binding experiments with B16F1 cells using ^{125}I-NDP-MSH as radioligand.

FIGURE 1 Schematic representation of MC1R-targeting with α-MSH analogs labeled with a radiometal.

high binding affinity and specificity to MC1 receptors have been labeled with radiohalogens (^{18}F, ^{123}I) or with radiometals (^{111}In, ^{99m}Tc, or ^{67}Ga). In the latter case, the α-MSH peptide analogs were previously linked to a bifunctional chelating agent (BFCA) appropriate for coordination to the metal. The resulting radiopeptides were expected to selectively bind the MC1 receptors overexpressed on the membrane of melanoma cells, being actively taken up through receptor–ligand internalization. The cellular internalization would promote the sequestering of the peptide-targeted radionuclide in the tumor cell's cytoplasm, leading to a higher accumulation of radioactivity in the tumor, compared to nontarget organs. Figure 1 depicts the MC1R melanoma-targeting approach based on a metal-labeled α-MSH peptide analog.

The most significant advances of peptide-MC1R radionuclide therapy of melanoma were recently reviewed.[13] Therefore, herein we will focus on radiolabeled α-MSH analogs developed and biologically evaluated for melanoma diagnosis, with particular emphasis on cyclic radiopeptides. Table II summarizes the binding affinity for MC1R (expressed as IC_{50} values) of α-MSH analogs and corresponding chelator–peptide conjugates. Tables III and IV summarize the most significant biodistribution data of promising radiolabeled-cyclized α-MSH analogs for single photon emission computed tomography (SPECT) and PET.

BIFUNCTIONAL CHELATORS AND RADIOISOTOPES EXPLORED FOR α-MSH ANALOGS

Radiopharmaceuticals for diagnosis contain gamma- or positron-emitting radionuclides being suitable for SPECT or PET, respectively.[14] When the radionuclides are the radiohalogens ^{18}F or ^{123}I, radiohalogenation can be performed either directly or via prosthetic groups, whose introduction into a peptide usually decreases dehalogenation but increases lipophilicity and consequently, hepatobiliary clearance.[5] This effect is not unexpected, because it is well known that lipophilic radiopeptides in general are predominantly metabolized by liver and excreted trough the hepatobiliary pathway.

The most used prosthetic groups for radiohalogenation of peptides, namely α-MSH analogs, are *N*-succinimidyl-4-^{125}I-iodobenzoate (^{125}I-PIB) or *N*-succinimidyl-4-^{18}F-fluorobenzoate (^{18}F-SFB).[5,15–17]

However, most of the radiotracers are metal-based complexes and the great majority of SPECT diagnostic radiopharmaceuticals currently available are either ^{99m}Tc complexes or target-specific biomolecules labeled with ^{99m}Tc or ^{111}In.[14] The preferential use of ^{99m}Tc, considered the workhorse of nuclear medicine, reflects its ideal nuclear properties ($t_{1/2}$ = 6.02 h; $E_{\gamma max}$ = 140 keV), low cost and availability from ^{99}Mo/^{99m}Tc commercial generators. Another relevant feature of ^{99m}Tc relates to its diverse and rich redox chemistry. Despite that, most of the ^{99m}Tc-radiopharmaceuticals in clinical use have the metal in the (V) oxidation state and contain the core $[^{99m}Tc(O)]^{3+}$. More recently, the remarkable features presented by the organometallic precursor *fac*-$[M(CO)_3(H_2O)_3]^+$ (M = Re(I), Tc(I)), introduced by Alberto et al.[18,19] brought renewed interest to the design of innovative low-oxidation ^{99m}Tc-based compounds. Indeed, the easy preparation of *fac*-$[M(CO)_3(H_2O)_3]^+$ directly from $[MO_4]^-$, the lability of the three water molecules and the chemical robustness of the *fac*-$[M(CO)_3]^+$ unit opened new avenues for the design of innovative Tc(I)-specific radiopharmaceuticals. Profiting from the availability of this new core, we have recently introduced a new family of bifunctional chelators, which combine a pyrazolyl unit with aliphatic amines, carboxylic acids, and/or thioethers, and we have explored their reactivity toward the *fac*-$[M(CO)_3]^+$ unit.[20–22] Such BFCAs, namely the one indicated in Figure 2A (pz1), were suitable for labeling biologically relevant molecules, namely bombesin analogs, linear and cyclic α-MSH analogs, and cyclic arginine-glycine-aspartate–based peptides.[23–28] Other research groups have also studied the labeling of peptides, namely α-MSH analogs, with other diagnostic radiometals (e.g., ^{111}In, ^{64}Cu, ^{68}Ga, and ^{86}Y), being 1,4,7,10-tetraazacyclododecane-1,4,7,10-tetracetic acid (DOTA; Figure 2B) the most explored and successful BFCA.[5,29] This chelator, despite forming very stable complexes with most of the referred metals,[5] leads quite often to high undesirable kidney uptake as is the case of a ^{111}In-labeled neuropeptide Y analog specific for the Y1-receptor.[30] In contrast, when the same neuropeptide Y analog was labeled with ^{99m}Tc(I) through conjugation to the N^{α}-histidinyl acetyl chelator, the resulting radiopeptide became a very promising imaging probe, since it gave clear SPECT images of breast cancer and metastasis in patients with low kidney uptake.[31] These and other results in the literature confirm the influence of the chelation chemistry and radiometal nature

Table III Most Relevant *in Vivo* Data for Some PET and SPECT Radiolabeled Metal-Based Cyclized α-MSH Analogs for Melanoma Imaging

Metal-Cyclized Radiopeptide: Name/Peptide Sequence (Metal Coordination Site in Bold)	Tumor Model	Time p.i. (h)	Tumor Uptake (%ID/g)	kidney Uptake (%ID/g)	Tumor/ Kidney Ratio	Tumor/ Blood Ratio	Tumor/ Muscle Ratio	Ref.
SPECT								
[^{99m}Tc]CCMSH	B16/F1 (m)	1	10.9 ± 0.5	22.6 ± 2.7	0.48	6.8	64	34
[^{99m}Tc](Ac-**CC**EHfRW**C**KPV-NH_2)								
[^{111}In]DOTA-Re-CCMSH	B16/F1 (m)	2	11.4 ± 2.9	8.98 ± 0.8	1.3	163	228	33
[^{111}In]DOTA-Re(**CC**EHfRW**C**KPV-NH_2)								
[^{111}In]DOTA-Re-CCMSH(Arg^{11})	B16/F1 (m)	2	17.3 ± 2.5	8.7 ± 1.3	2.0	16	576	36
[^{111}In]DOTA-Re-(**CC**EHfRW**C**RPV-NH_2)								
[^{99m}Tc]CCMSH(Arg^{11})	B16/F1 (m)	1	14.0 ± 2.6	11.7 ± 1.4	1.2	16	61	37
[^{99m}Tc](Ac-**CC**EHfRW**C**RPV-NH_2)								
Ac-DLys([^{125}I]IBA)-Re-CCMSH(Arg^{11})	B16/F1 (m)	4	15.1 ± 1.4	8.6 ± 0.87	1.7	6.3	59.9	15
Ac-k([^{125}I]-IBA)								
Re-(**CC**EHfRW**C**RPV-NH_2)								
PET								
[^{86}Y]DOTA-Re-CCMSH(Arg^{11})	B16/F1 (m)	2	9.83 ± 2.27	18.6 ± 3.6	0.53	164	164	38
[^{86}Y]DOTA-Re(**CC**EHfRW**C**RPV-NH_2)								
[^{64}Cu]DOTA-Re-CCMSH(Arg^{11})	B16/F1 (m)	2	8.8 ± 1.7	9.88 ± 1.26	0.89	12	18	38
[^{64}Cu]DOTA-Re(**CC**EHfRW**C**RPV-NH_2)								
[^{64}Cu]CBTE2A-Re-CCMSH(Arg^{11})	B16/F1 (m)	2	7.1 ± 3.2	8.6 ± 2.5	0.83	37	44	39
[^{64}Cu]CBTE2A-Re(**CC**EHfRW**C**RPV-NH_2)								
[^{68}Ga]DOTA-Re-CCMSH(Arg^{11})	B16/F1 (m)	2	4.25 ± 1.41	6.8 ± 1.72	0.62	11	43	41
[^{68}Ga]DOTA-Re(**CC**EHfRW**C**RPV-NH_2)								
Low specific activity								
[^{68}Ga]DOTA-Re-CCMSH(Arg^{11})	B16/F1 (m)	1	6.27 ± 1.6	5.45 ± 0.72	1.1	14	89	42
[^{68}Ga]DOTA-Re(**CC**EHfRW**C**RPV-NH_2)								
High specific activity								
Ac-*D*Lys([^{18}F]-FB)-Re-CCMSH(Arg^{11})	B16/F10 (m)	2	2.11 ± 0.12	5.42 ± 0.50	0.39	2.59	7.43	16
Ac-k([^{18}F]-FB)Re-			1.36 ± 0.18	17.8 ± 1.80	0.07	3.49	7.01	
(**CC**EHfRW**C**RPV-NH_2)Isomer 1/Isomer 2								
	A375 (h)	2	0.33 ± 0.04	5.02 ± 0.10	0.06	0.77	1.57	16
			0.42 ± 0.19	16.9 ± 2.9	0.02	1.98	2.53	

Table IV Most Relevant *in Vivo* Data for Some SPECT Radiolabeled Lactam Bridge-based Cyclized α-MSH Analogs for Melanoma Imaging

Lactam-Cyclized Radiopeptide: Name/Peptide Sequence	Tumor Model	Time p.i. (h)	Tumor Uptake (%ID/g)	kidney Uptake (%ID/g)	Tumor/ Kidney Ratio	Tumor/ Blood Ratio	Tumor/ Muscle Ratio	Ref.
[^{99m}Tc]pz1-βAlaMT-II [^{99m}Tc]pz1-βAla-Nle-c(DHfRWK)	B16/F1 (m)	4	11.3 ± 1.8	32.1 ± 1.6	0.35	6.8	61.4	27
[^{111}In]DOTA-CycMSH [^{111}In]DOTA-c(K-Nle-EHfRWGRPVD)	B16/F1 (m)	2	9.5 ± 1.4	16.2 ± 1.9	0.59	106	68	45
[^{111}In]DOTA-GlyGlu-CycMSH [^{111}In]DOTA-GE-c(K-Nle-EHfRWGRPVD)	B16/F1 (m)	2	10.4 ± 1.4	13.1 ± 2.5	0.8	74	173	45
Ac-GluGlu-CycMSH[DOTA]-^{111}In Ac-EE-c(K-Nle-EHfRWGRPVK(DOTA))^{111}In	B16/F1 (m)	2	11.4 ± 2.2	60.5 ± 8.4	0.19	54	95	47
[^{67}Ga]DOTA-Gly-Glu-CycMSH [^{67}Ga]DOTA-GE-c(K-Nle-EHfRWGRPVD)	B16/F1 B16/F10 (m)	2	12.9 ± 1.6	27.5 ± 7.9	0.46	258	323	48

on the radiopeptide tumor targeting properties and pharmacokinetic profile.[5,14]

Another bifunctional chelator recently introduced for labeling α-MSH analogs with ^{64}Cu was 4,11-bis(carboxymethyl)-1,4,8,11-tetraazabicyclo[6,6,2]hexadecane (CBTE2A; Figure 2C).[32] As will be discussed in metal-cyclization section, this chelator allowed the complexation of ^{64}Cu with improved in vivo stability and clearance, compared to DOTA.

CYCLIC RADIOLABELED α-MSH ANALOGS FOR MELANOMA IMAGING

Cyclization of α-MSH analogs has been used to improve binding affinity, in vivo stability, and receptor selectivity.[10] In comparison with their linear counterparts, stabilization of secondary structures such as β-turns make the cyclic peptides less flexible in conformation and with a better fit receptor binding pocket, enhancing their binding affinities.[10] Cyclization strategies include backbone to backbone, N-terminus to C-terminus, one side chain to C-terminus or N-terminus, two side chains via disulfide or lactam bridges, and metal coordination based.[10] Among these, the disulfide-, lactam-, and metal-based cyclizations have been the most explored in the case of radiolabeled α-MSH analogs.[5,13,27]

Disulfide Bridge Cyclization

α-MSH peptides cyclized via disulfide bonds such as the case of CMSH (Tables I and II) display increased receptor-binding affinity and resistance to proteolysis. CMSH was conjugated to DOTA (DOTA–CMSH: IC_{50} = 1.6 ± 0.3 n*M*), labeled with ^{111}In, and the contribution of cyclization on in vivo melanoma targeting evaluated and compared with the corresponding linear- and metal-based cyclic peptide analogs (see metal cyclization section).[33] The disulfide-bond cyclized radiopeptide ^{111}In-DOTA-CMSH presented a moderate tumor uptake (7.5 ± 1.0% injected dose (ID)/g) and a high kidney accumulation (38.4 ± 3.6%ID/g) at 2 h postinjection

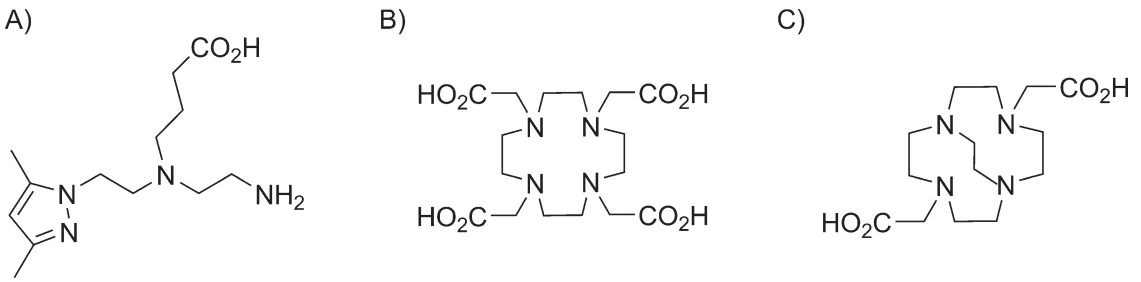

FIGURE 2 Chemical structure of BFCAs used in the radiolabeling of α-MSH analogs. (A) pz1 (4-{(2-aminoethyl)[2-(3,5-dimethyl-1H-pyrazoly-1-yl)ethyl]amino} butanoic acid), (B) 1,4,7,10-tetraazacyclododecane-1,4,7,10-tetraacetic acid (DOTA), and (C) 4,11,bis(carboxymethyl)-1,4,8,11-tetraazabicyclo6,6,2hexadecane (CBTE2A).

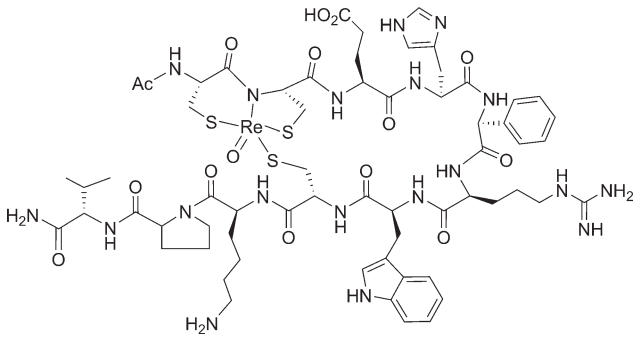

FIGURE 3 Structure of Ac-ReCCMSH.

(p.i.) in B16F1 murine melanoma-bearing mice.[33] The decreased tumor uptake (5.9 ± 1.9%ID/g at 2 h p.i.) exhibited by the corresponding linear radiopeptide underlined the benefit of peptide cyclization. Furthermore, considering the two cyclized radiopeptides, better melanoma-targeting properties and kidney clearance were obtained for metal cyclization (see metal cyclization section), relatively to disulfide-bond cyclization.[33]

Metal Cyclization

α-MSH analogs cyclized through site-specific rhenium (Re) and technetium (Tc) metal coordination were structurally characterized and their ability to bind melanoma cells described.[34] The Re-peptide complex Re-[$Cys^{3,4,10}$,*D*Phe^{7}]-α-$MSH_{3–13}$ (ReCCMSH), where the metal is stabilized by three $Cys^{3,4,10}$ sulfhydryls and one Cys^{4} amide nitrogen, displayed a receptor-binding affinity of 2.9 n*M* (Figure 3 and Table II).

This metal-based cyclization makes the peptide not only very resistant to chemical and proteolytic degradation but also highly bioactive. The rhenium-free analog, CCMSH, was directly radiolabeled and cyclized by coordination to ^{99m}Tc.[34] Despite the high kidney uptake (22.6 ± 2.7%ID/g, 1 h p.i.), the ability of ^{99m}Tc-CCMSH to target B16F1-melanoma (10.9 ± 0.5%ID/g for tumor uptake at 1 h p.i.) became the proof-of-principle of the potential use of metal-cyclized radiolabeled compounds for melanoma imaging or therapy.[34] In further studies, DOTA was conjugated to the amino terminus of the metal-cyclized complex Re-CCMSH (IC_{50} = 1.2 n*M*) and to the linear analog CCMSH (IC_{50} = 4.9 n*M*) and the resulting conjugates were labeled with ^{111}In.[33] The rhenium-cyclized radiopeptide ^{111}In-DOTA-Re-CCMSH presented increased in vivo tumor-targeting capacity (11.4 ± 2.9%ID/g, at 2 h p.i.) and high tumor retention (4.9 ± 1.5%ID/g, at 24 h p.i.) in murine melanoma-bearing mice, compared with the linear analog ^{111}In-DOTA-CCMSH (tumor uptake: 5.9 ± 1.9%ID/g and 1.9 ± 0.6%ID/g at 2 and at 24 h p.i., respectively).

A general limitation of most radiopeptides is the nonspecific kidney accumulation with subsequent radionephrotoxicity in therapeutic applications. As mentioned earlier, this problem is often associated to DOTA-peptide conjugates. In the case of Re-mediated cyclization, an enhanced renal clearance was observed for the cyclic ^{111}In-DOTA-Re-CCMSH (e.g., 8.89 ± 0.8%ID/g at 2 h p.i.), being the value six to eight times lower than that of the linear ^{111}In-DOTA-CCMSH. By comparing the two metal-based cyclized CCMSH analogs, ^{111}In-DOTA-Re-CCMSH *versus* ^{99m}Tc-CCMSH, similar tumor uptake was found, but the Re-mediated cyclized radiopeptide presented an enhanced whole-body clearance and a higher tumor-to-blood ratio (163 *vs.* 6.8, Table III).[35] Despite these favorable features, a relatively high level of radioactivity still remained in the kidneys in the case of ^{111}In-DOTA-Re-CCMSH. Thus, to reduce kidney uptake, four new ^{111}In-DOTA-derivatized Re-CCMSH analogs were prepared and

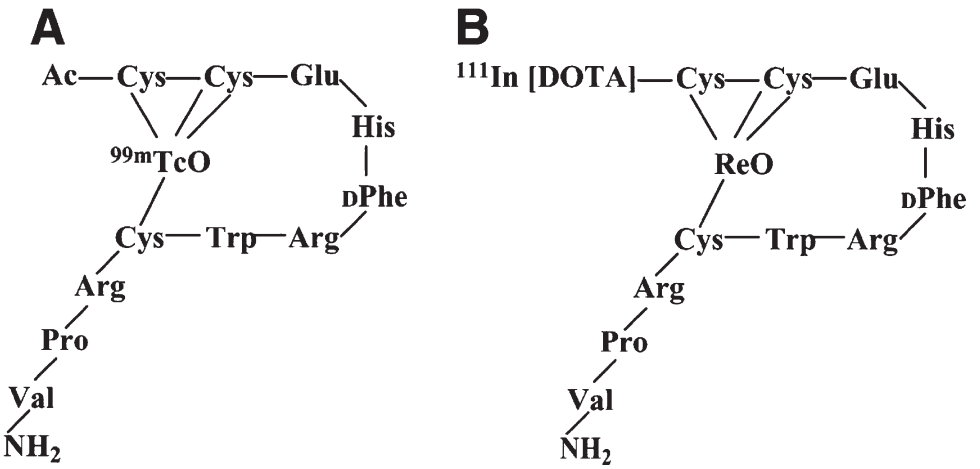

FIGURE 4 Schematic structures of ^{99m}Tc-(Arg^{11})CCMSH (A) and ^{111}In-DOTA-Re(Arg^{11})CCMSH (B).

their biological profile evaluated in murine melanoma model.[36] Among them, the analog ^{111}In-DOTA-Re-CCMSH(Arg^{11}) (Lys^{11} replaced by Arg, Figure 4B) showed the highest tumor uptake (17.3 ± 2.5%ID/g) and lowest kidney radioactivity accumulation (8.7 ± 1.3%ID/g) at 2 h p.i.[36] The analog CCMSH(Arg^{11}) was also cyclized through the labeling with ^{99m}Tc, and the MC1R-targeting properties of the resulting complex ^{99m}Tc-CCMSH(Arg^{11}) (Figure 4A) were compared with those of ^{99m}Tc-CCMSH and ^{111}In-DOTA-Re-CCMSH(Arg^{11}).[37]

Also in this case, the replacement of Lys^{11} by Arg improved tumor uptake (^{99m}Tc-CCMSH(Arg^{11}): 14.0 ± 2.6%ID/g; ^{99m}Tc-CCMSH: 10.9 ± 0.5%ID/g) and reduced kidney accumulation (^{99m}Tc-CCMSH(Arg^{11}): 11.7 ± 1.4%ID/g; ^{99m}Tc-CCMSH: 22.6 ± 2.7%ID/g) at 1 h p.i.. Comparatively to the Re-cyclized analog ^{111}In-DOTA-Re(Arg^{11})CCMSH, the ^{99m}Tc-CCMSH(Arg^{11}) complex exhibited favorable and comparable tumor targeting properties. Both ^{111}In-Re- and ^{99m}Tc-cyclized radiopeptides allowed clear micro-SPECT/CT images of flank melanoma tumors as well as of B16F10 pulmonary melanoma metastases, with ^{99m}Tc-CCMSH(Arg11) presenting images with greater resolution of metastatic lesions.[37]

Efforts to develop radio-iodinated linear α-MSH analogs for melanoma targeting were disappointing, mainly because of slow clearance and in vivo deiodination. Nevertheless, the radioiodinated analog Ac-D-Lys(^{125}I-4-iodobenzoate)-ReCCMSH(Arg^{11}) exhibited a rapid clearance from normal tissues and a significantly higher B16F1-melanoma uptake (15.1 ± 1.4%ID/g, at 4 h p.i.) and retention (7.2 ± 2.1%ID/g, at 24 h p.i.) than the radio-iodinated linear NDP peptide.[15] The tumor uptake of this radio-iodinated peptide was comparable to that of ^{111}In-DOTA-Re-CCMSH(Arg^{11}).

For PET imaging, the DOTA-Re-CCMSH(Arg^{11}) analog was labeled with ^{64}Cu and ^{86}Y.[38] ^{64}Cu-DOTA-Re-CCMSH(Arg^{11}) presented a high radioactivity accumulation in nontarget organs (e.g., blood, liver, and kidney), most likely due to the in vivo instability of the complex and consequent release of ^{64}Cu. To avoid this problem, the DOTA chelator was replaced by CBTE2A, which is known to form Cu^{2+}-complexes with high stability and kinetic inertness. As shown in Table II, the MC1R binding properties of CBTE2A-Re-CCMSH(Arg11) were kept unchanged, as indicated by its MC1R binding affinity value (IC_{50} = 5.4 n*M*), similar to the one obtained for DOTA-Re-CCMSH(Arg^{11}) (IC_{50} = 6.9 nM).[39] The radioactive complex ^{64}Cu-CBTE2A-Re-CCMSH(Arg^{11}) presented a B16F1 melanoma uptake (7.1 ± 3.2%ID/g at 2 h p.i.) comparable with ^{64}Cu-DOTA-Re-CCMSH(Arg^{11}) but a much lower nontarget organs accumulation, yielding significantly higher tumor-to-nontarget tissue ratios. Among PET candidates, the superiority of ^{64}Cu-CBTE2A-Re-CCMSH(Arg^{11}) over ^{86}Y-DOTA-Re-CCMSH(Arg^{11}) has been demonstrated by the increased tumor retention and kidney clearance. The linear ^{64}Cu-DOTA-NAPamide,[40] with low tumor uptake and high radioactivity accumulation in nontarget organs, did not present advantages over the cyclized Re-CCMSH(Arg^{11}) radio analogs.

Because the use of ^{68}Ga-labeled peptides is an emerging area of PET radiopharmaceutical research, ^{68}Ga-DOTA-Re-CCMSH(Arg^{11}) with low and high specific activity was prepared and evaluated.[41,42] Despite some differences in the biological profile (Table III), in both cases the tumor uptake was still low when compared with the linear α-MSH analog ^{68}Ga-DOTA-NAPamide in the same in vivo melanoma model (9.4 ± 1.1%ID/g and 3.98 ± 0.10%ID/g at 4 h p.i. for tumor and kidney uptake, respectively). Such results indicated that the Re-mediated cyclization did not bring significant advantages when the radiometal is ^{68}Ga.[11,42]

Still for PET imaging, the two isomers of Ac-*D*Lys-Re-CCMSH(Arg^{11}) were labeled using ^{18}F-SFI.[16] Binding affinity for the inactive-fluorinated isomeric compounds were in the nanomolar range (5.7 and 9.0 n*M*). However, the best ^{18}F-isomer displayed a relatively low murine melanoma uptake (2.1 ± 0.1%ID/g) and moderate kidney (5.4 ± 0.5%ID/g), lung (2.4 ± 0.6%ID/g), and liver (2.4±0.4%ID/g) radioactivity accumulation at 2 h p.i. Despite the suboptimal low tumor uptake and retention found for the ^{18}F-labeled cyclic α-MSH analog, these values were still higher than those obtained for the linear ^{18}F-NDP and ^{18}F-NAPamide.[17] Again, the advantages of the metal (Re)-based cyclization as a scaffold for developing a MC1R PET based on ^{18}F-agents are not evident. To take advantage of the higher sensitivity of PET over SPECT, further optimization will be needed for PET MC1R-targeting with linear and cyclic peptides.

Lactam Bridge Cyclization

We have reported a novel class of α-MSH analogs cyclized through a side chain lactam bridge, based on Melanotan II (MT-II) (Table I).[27] The cyclic peptide *β*Ala-Nle-*c*[Asp-His-*D*Phe-Arg-Trp-Lys]-NH_2 (*β*AlaMT-II) and its linear counterpart, named MSHoct, (Table I) were conjugated to the bifunctional chelator agent pz1 (Figure 2A).[27,43] Lactam cyclization resulted in a compact structure with a remarkable enhancement of binding affinity. The cyclic pz1-peptide conjugate, pz1-*β*AlaMT-II, displayed a higher binding affinity to MC1R (IC_{50} = 0.21 n*M*) than the corresponding linear conjugate pz1-MSHoct (IC_{50} = 1.25 n*M*) (Table II; Raposinho et al., unpublished results). Both cyclic and linear pz1-peptide conjugates were labeled with *fac*-[^{99m}Tc(CO)$_3$]$^+$ and the corresponding radiopeptides ^{99m}Tc-(CO)$_3$-pz1-*β*AlaMT-II and ^{99m}Tc-(CO)$_3$-

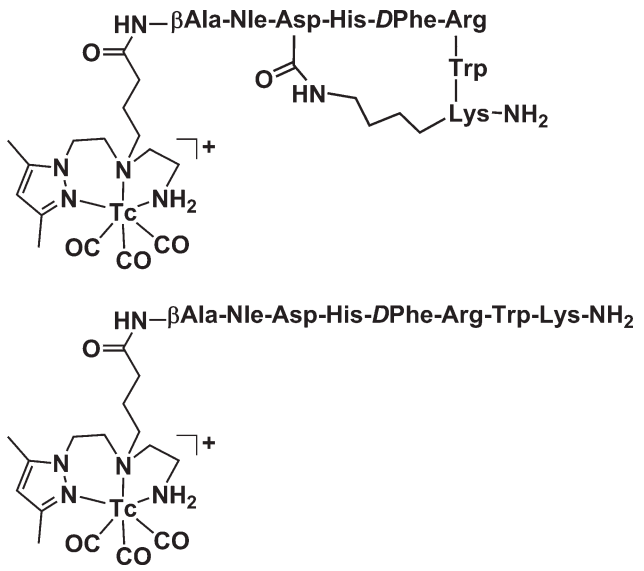

FIGURE 5 Structure of ^{99m}Tc-$(CO)_3$-pz1-βAlaMT-II and ^{99m}Tc-$(CO)_3$-pz1-MSHoct.

pz1-MSHoct (see Figure 5) were evaluated for their potential as melanoma imaging probes in murine melanoma model.[27]

The lactam-cyclized radioconjugate, ^{99m}Tc-$(CO)_3$-pz1-βAlaMT-II, presented remarkable internalization in B16F1 cells (50.5% of total applied activity, 4 h at 37°C) compared with the values found for the linear radiopeptide (1.6% of total applied activity) under similar conditions.[27] The internalization/retention level of ^{99m}Tc-$(CO)_3$-pz1-βAlaMT-II was also particularly high when compared with other radiolabeled cyclic α-MSH analogs, namely ^{99m}Tc-CCMSH.[44] In B16F1 melanoma-bearing mice, ^{99m}Tc-$(CO)_3$-pz1-βAlaMT-II (11.3 ± 1.8%ID/g) has shown a significant tumor uptake, compared with ^{99m}Tc-$(CO)_3$-pz1-MSHoct (1.0 ± 0.1%ID/g) at 4 h p.i., and this accumulation was MC1R-mediated, as indicated by receptor-blocking studies in the presence of the potent NDP-αMSH agonist.[27] However, the clearance from the excretory organs (liver and kidney) as well as the overall excretion rate were negatively affected by cyclization.[27] The same strategy, using the pz1 chelator, has been also applied by us to the labeling of the linear α-MSH analog NAPamide with ^{99m}Tc(I).[26] The resulting linear radiopeptide ([Ac-Nle^4,Asp^5,*D*Phe^7, Lys^{11}(pz1-^{99m}Tc$(CO)_3$)α-MSH_{4-11} presented a better pharmacokinetic profile but the tumor-targeting properties were not as favorable as those observed for the ^{99m}Tc-labeled lactam-cyclized peptide. Indeed, besides a lower cellular internalization and retention in melanoma cells, the tumor uptake values for the linear ^{99m}Tc-NAPamide at 1 and 4 h p.i. were only 63.5% and 37.5%, respectively, of those obtained for the cyclic radiopeptide.[26,27] Furthermore, the tumor uptake of the ^{99m}Tc-labeled lactam-based cyclized peptide was comparable to that obtained for the previously described ^{99m}Tc-labeled metal-based cyclized peptides ^{99m}Tc-CCMSH (9.5 ± 2.0%ID/g at 4 h p.i.) and ^{99m}Tc-CCMSH(Arg^{11}) (11.2 ± 1.7%ID/g) at 4 h p.i.[34,36] Thus, despite the promising tumor-targeting properties, the pharmacokinetic profile of the cyclic ^{99m}Tc-$(CO)_3$-pz1-βAlaMT-II has still to be improved to increase the overall excretion rate and to decrease radioactivity retention in the excretory organs. Taking into account the few number of reported ^{99m}Tc-labeled α-MSH analogs together with the interest on designing new ^{99m}Tc radioactive probes for melanoma imaging, tuning of the pharmacokinetic profile of ^{99m}Tc-$(CO)_3$-pz1-βAlaMT-II deserves significant research effort, being a challenging task in the future.

The influence of lactam bridge-based cyclization on melanoma targeting was also explored by Miao et al.[45], using two longer cyclic α-MSH analogs. DOTA-CycMSH (Figure 6A) and DOTA-GlyGlu-CycMSH (Figure 6B) conjugates displayed IC_{50} values of 1.75 and 0.9 n*M*, respectively (Table II).

In B16F1 melanoma-bearing mice, both ^{111}In-labeled conjugates exhibited high receptor-mediated tumor uptake (^{111}In-DOTA-CycMSH: 9.5 ± 1.4%ID/g; ^{111}In-DOTA-GlyGlu-CycMSH: 10.4 ± 1.4%ID/g, at 2 h p.i.). These values were comparable with those found for the lactam bridge–cyclized α-MSH analog ^{99m}Tc-pz1-βAlaMT-II, described before, and for the metal-cyclized ^{111}In-DOTA-Re-CCMSH (11.4 ± 2.89%ID/g), but slightly lower and higher than those found for ^{111}In-DOTA-Re-CCMSH(Arg^{11}) (17.29 ± 2.49%ID/g) and for the disulfide bridge–cyclized α-MSH peptide ^{111}In-DOTA-CMSH (7.51 ± 2.89%ID/g) (Tables II and III), respectively.[27,33,35] The accumulation of ^{111}In-DOTA-CycMSH and ^{111}In-DOTA-GlyGlu-CycMSH in non-target organs was in general low, except in kidneys (21.69 ± 0.34 and 12.13 ± 1.17%ID/g, respectively, at 4 h p.i.). Intro-

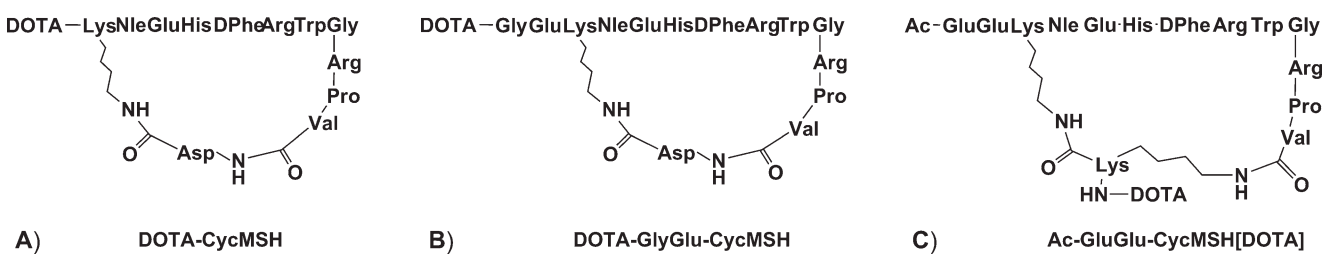

FIGURE 6 Schematic structures of DOTA-lactam-cyclized α-MSH analogs.

duction of a negatively charged linker (-Gly-Glu-) into the peptidic sequence (^{111}In-DOTA-GlyGlu-CycMSH) decreased the renal uptake by 44%, without affecting the tumor accumulation. However, the activity in kidney was still 29% higher than that found for ^{111}In-DOTA-Re-CCMSH, and 34% of that of ^{111}In-DOTA-CMSH, indicating that lactam cyclization led to lower kidney accumulation than the disulfide one.[33,35]

It is known that the nature and position of the chelator may significantly affect the tumor-targeting properties and pharmacokinetic profile. Such effect was found for linear and for lactam bridge–cyclized α-MSH peptides. The introduction of the DOTA chelator at the N terminus of the linear peptide NAPamide or on the side-chain amino group of Lys^{11} influenced differently the MC1 receptor binding affinity ($IC_{50} = 2.13 \pm 0.29$ n*M* vs. 1.19 ± 0.19 n*M*, $P < 0.05$), as well as the melanoma and kidney radioactivity accumulation of ^{111}In-labeled conjugates.[46] To evaluate the effect of DOTA position in ^{111}In-labeled lactam bridge–cyclized α-MSH peptides, the chelator was conjugated to the Lys in the cyclic ring, and the N-terminus was acetylated, to generate the conjugate AcGluGlu-CycMSH[DOTA] (Figure 6C).[47] This conjugate presented the best IC_{50} value (0.6 n*M*) among the derivatives of CycMSH previously studied.[45,47] However, despite the good affinity to MC1R, high tumor uptake (11.4 ± 2.2%ID/g, 2 h p.i.) and prolonged tumor retention (9.4 ± 2.4%ID/g, 4 h p.i.), the overall pharmacokinetic profile of AcGluGlu-CycMSH[DOTA]^{111}In was not favorable because of the high kidney uptake (60.5 ± 8.4%ID/g at 2 h p.i.).[47] The kidney and liver uptake of AcGluGlu-CycMSH[DOTA]^{111}In were 5.5 and 6.1 times higher than the corresponding uptake of ^{111}In-DOTA-GlyGlu-CycMSH at 4 h p.i.

The cyclic DOTA-Gly-Glu-cMSH conjugate (apparently the best of CycMSH conjugates) was recently labeled with ^{67}Ga.[48] The radiocompound ^{67}Ga-DOTA-GlyGlu-CycMSH exhibited high tumor uptake (12.93 ± 1.63%ID/g, at 2 h p.i.) and prolonged tumor retention (5.02 ± 1.35%ID/g at 24 h p.i.) in B16/F1 melanoma-bearing mice. Uptake of ^{67}Ga-DOTA-GlyGlu-CycMSH were generally very low for nontarget organs (<0.30%ID/g) except for the kidneys (27.55 ± 7.87%ID/g at 4 h p.i.). Both flank primary B16/F1 melanoma and B16/F10 pulmonary melanoma metastases were clearly visualized by SPECT/CT imaging using ^{67}Ga-DOTA-GlyGlu-CycMSH as the radioactive probe.[48]

CONCLUDING REMARKS AND PERSPECTIVES

The described data brought together have shown that the nature of the bifunctional chelator and radiometal used affected the biodistribution and excretion properties of the radiopeptides. Furthermore, the different strategies of cyclization described herein yielded molecules with different in vivo tumor uptake and pharmacokinetic profile, being the disulfide-bond cyclization strategy the less promising. High MC1R binding affinity, efficient cellular internalization and extended retention, high receptor-mediated tumor uptake, highlighted the potential of radiolabeled lactam bridge-cyclized α-MSH peptide analogs for melanoma imaging and/or therapy. This new class of cyclic radiopeptides became a good alternative to the ^{99m}Tc/^{111}In-labeled Re-CCMSH cyclized analogs in the development of novel radiopeptides for MC1R-targeting. The most promising radiolabeled MC1R-targeting peptides reported showed high tumor uptake and good imaging properties in B16F1 murine melanoma-bearing mice. However, further improvement of pharmacokinetics, namely reduction of renal uptake is still needed to facilitate the clinical evaluation of this class of radiolabeled α-MSH peptides as melanoma imaging probes or therapeutic agents. It must also be emphasized that the tumor model used for the evaluation of radiolabeled α-MSH analogs leads to an overestimation of the accumulation expected in humans. Indeed, the MC1 receptor density varies among the different murine and human melanoma cells lines, from several hundred to around 10,000 receptors per cell, with the murine B16F1 cells showing 6- to 15-fold higher density than most human melanoma cell lines.[8,49–51] A few radiolabeled α-MSH analogs have also been evaluated in the human A375 melanoma xenografts, where low tumor uptake values were obtained. However, this human model is one of the most unfavorable human models as the MC1R expression in A375 cells is rather low. Therefore, the best radiolabeled imaging probes in murine melanoma model should be further evaluated in different and more representative human melanoma models.

REFERENCES

1. Jemal, A.; Siegel, R.; Ward, E.; Hao, Y.; Xu, J.; Thun, M. J. CA Cancer J Clin 2009, 59, 225–249.
2. Gray-Schopfer, V.; Wellbrook, C.; Marais, R. Nature 2007, 445, 851–857.
3. Belhocine, T. Z.; Scott, A. M.; Even-Sapir, E.; Urbain, J. L.; Essner, R. J Nucl Med 2006, 47, 957–967.
4. Choi, E. A.; Gershenwald, J. E. Surg Oncol Clin N Am 2007, 16, 403–430.
5. Schottelius, M.; Wester, H.-J. Methods 2009, 48, 161–177.
6. Reubi, J. C.; Maecke, H. R. J Nucl Med 2008, 49, 1735–1738.
7. Ghanem, G. E.; Comunale, G.; Libert A.; Vercammen-Grandjean, A.; Lejeune, F. J. Int J Cancer 1988, 41, 248–255.
8. Siegrist, W.; Solca, F.; Stutz, S.; Giuffre, L.; Carrel, S.; Girard, J.; Eberle A. N. Cancer Res 1989, 49, 6352–6358.
9. Siegrist, W.; Stutz, S.; Eberle, A. N. Cancer Res 1994, 54, 2604–2610.

10. Holder, J. R.; Haskell-Luevano, C. Med Res Rev 2004, 24, 325–356.
11. Froidevaux, S.; Calame-Christe, M.; Shuhmacker, J.; Tanner, H.; Saffrich, R.; Henze, M.; Eberle, A. N. J Nucl Med, 2004, 45, 116–123.
12. Cody, W. L.; Mahoney, M.; Knittle, J. J.; Hruby, V. J.; Castrucci, A. M.; Hadley, M. E. J Med Chem 1985, 28, 583–588.
13. Miao, Y.; Quinn, T. P. Crit Rev Oncol/Hematol 2008, 67, 213–228.
14. Liu, S. Adv Drug Deliv Rev 2008, 60, 1347–1370.
15. Cheng, Z.; Chen, J.; Quinn, T. P.; Jurisson, S. S. Cancer Res 2004, 64, 1411–1418.
16. Ren, G.; Liu, Z.; Miao, Z.; Liu, H.; Subbarayan, M.; Chin, F. T.; Zhang, L.; Gambhir, S. S.; Cheng, Z. J Nucl Med, 2009, 50, 1865–1872.
17. Cheng, Z.; Zhang, L.; Graves, E.; Xiong, Z.; Dandekar, M.; Chen, X.; Gambhir, S. S. J Nucl Med 2007, 48, 987–994.
18. Alberto, R.; Schibli, R.; Egli, A.; Schubiger, A. P.; Abram, U.; Kaden, T. A. J Am Chem Soc 1998, 120, 7987–7988.
19. Alberto, R. Eur J Inorg Chem 2009, 1, 21–31.
20. Alves, S.; Paulo, A.; Correia, J. D. G.; Domingos, Â.; Santos, I. J Chem Soc Dalton Trans 2002, 24, 4714–4719.
21. Vitor, R.; Alves, S.; Correia, J. D. G.; Paulo, A.; Santos, I. J Organometallic Chem 2004, 689, 4764–4774.
22. Fernandes, C.; Santos, I. C.; Santos, I.; Pietzsch, H.-J.; Rey, J.; Margaritis, N.; Bourkoula, A.; Chiotellis, A.; Paravatou, M.; Pirmettis, I. Dalton Trans 2008, 24, 3215–3225.
23. Alves, S.; Paulo, A.; Correia, J. D. G.; Gano, L.; Smith, C. J.; Hoffman, T. J.; Santos, I. Bioconjug Chem 2005, 16, 438–449.
24. Alves, S.; Correia, J. D. G.; Santos, I.; Veerendraa, B.; Sieckman, G. L.; Hoffman, T. J.; Rold, T. L.; Figueroa, S. D.; Retzloff, L.; McCratea, J.; Prasanphanich, A.; Smith, C. J. Nucl Med Biol 2006, 33, 625–634.
25. Alves, S.; Correia, J. D. G.; Gano, L.; Rold, T. L.; Prasanphanich, A.; Haubner, R.; Rupprich, M; Alberto, R.; Decristoforo, C.; Santos, I.; Smith, C. J. Bioconjug Chem 2007, 18, 530–537.
26. Raposinho, P. D.; Correia, J. D. G.; Alves, S.; Botelho, M. F.; Santos, A. C.; Santos, I. Nucl Med Biol 2008, 35, 91–99.
27. Raposinho, P. D.; Xavier, C.; Correia, J. D. G.; Falcão, S.; Gomes, P.; Santos, I. J Biol Inorg Chem 2008, 13, 449–459.
28. Correia, J. D. G; Paulo, A.; Santos, I. Curr Radiopharm 2009, 2, 277–294.
29. Peterson, J. J.; Pak, R. H.; Meares, C. F. Bioconjug Chem 1999, 10, 316–320.
30. Zwanziger, D.; Khan, I. U.; Neundorf, I.; Sieger, S.; Lehmann, L.; Friebe, M.; Dinkelborg, L.; Beck-Sickinger, A. G. Bioconjug Chem 2008, 19, 1430–1438.
31. Khan, I. U.; Zwanziger, D.; Böhme, I.; Javed, M.; Naseer, H.; Hyder, S. W.; Beck-Sickinger, A. G. Angew Chem Int Ed Engl 2010, 49, 1155–1158.
32. Wong, E. H.; Weisman, G. R.; Hill, D. C.; Reed, D. P.; Rogers, M. E.; Condon, J. S.; Fagan, M. A.; Calabrese, J. C.; Lam, R. C.; Guzer, I. A.; Reingold, A. L. J Am Chem Soc 2000, 122, 10561–10572.
33. Chen, J.-Q.; Cheng, Z.; Owen, N. K.; Hoffman, T. J.; Miao, Y.; Jurisson, S. S.; Quinn, T. P. J Nucl Med 2001, 42, 1847–1855.
34. Giblin, M.F.; Wang, N.; Hoffman, T. J.; Jurisson, S. S.; Quinn, T. P. PNAS 1998, 95, 12814–12818.
35. Chen, J.-Q.; Cheng, Z.; Miao, Y.; Jurisson, S. S.; Quinn, T. P. Cancer 2002, 94, 1196–1201.
36. Cheng, Z.; Chen, J.; Miao, Y.; Owen, N. K.; Quinn, T. P.; Jurisson, S. S. J Med Chem 2002, 45, 3048–3056.
37. Miao, Y.; Benwell, K.; Quinn, T. P. J Nucl Med 2007, 48, 73–80.
38. McQuade, P.; Miao, Y.; Yoo, J.; Quinn, T. P.; Welch, M. J.; Lewis, J. S. J Med Chem 2005, 48, 2985–2992.
39. Wei, L.; Butcher, C.; Miao, Y.; Gallazzi, F.; Quinn, T. P.; Welch, M. J.; Lewis, J. S. J Nucl Med 2007, 48, 64–72.
40. Cheng, Z.; Xiong, Z.; Subbarayan, M.; Chen, X.; Gambhir, S. S. Bioconjug Chem 2007, 18, 765–772.
41. Wei, L.; Miao, Y.; Gallazzi, F.; Quinn, T. P.; Welch, M. J.; Vavere, A. L.; Lewis, J. S. Nucl Med Biol 2007, 34, 945–953.
42. Cantorias, M. V.; Figueroa, S. D.; Quinn, T. P.; Lever, J. R.; Hoffman, T. J.; Watkinson, L. D.; Carmack, T. L.; Cutler, C. S. Nucl Med Biol 2009, 36, 505–513.
43. Valldosera, M.; Monso, M.; Xavier, C.; Raposinho, P.; Correia, J. D. G.; Santos, I.; Gomes, P. Int J Pept Res Ther 2008, 14, 273–281.
44. Chen, J.-Q.; Chen, Z.; Hoffman, T. J.; Jurisson, S. S.; Quinn, T. P. Cancer Res 2000, 60, 5649–5658.
45. Miao, Y.; Gallazzi, F.; Guo, H.; Quinn, T. P. Bioconjug Chem 2008, 19, 539–547.
46. Froidevaux, S.; Calame-Christe, M.; Tanner, H.; Eberle, A. N. J Nucl Med 2005, 46, 887–895.
47. Guo, H.; Yang, J.; Gallazzi, F.; Prossnitz, E. R.; Sklar, L. A.; Miao, Y. Bioconjug Chem 2009, 20, 2162–2168.
48. Guo, H.; Yang, J.; Shenoy, N.; Miao, Y. Bioconjug Chem 2009, 20, 2356–2363.
49. Roberts, D. W.; Newton, R. A.; Beaumont, K. A.; Leonard, J. H.; Strum, R. A. Pigment Cell Res 2005, 19, 76–89.
50. Tatro, J. B.; Atkins, M.; Mier, J. W.; Hardarson, S.; Wolfe, H.; Smith, T.; Entwistle, M. L.; Reichlin, S. J Clin Invest 1990, 85, 1825–1832.
51. Miao, Y.; Whitener, D.; Feng, W.; Owen, N. K.; Chen, J. Q.; Quinn, T. P. Bioconjug Chem 2003, 14, 1177–1184.